

Non-Linear Phase-Shifting of Haar Wavelets for Run-Time All-Frequency Lighting

Mais Alnasser and Hassan Foroosh

Abstract

This paper focuses on real-time all-frequency image-based rendering using an innovative solution for run-time computation of light transport. The approach is based on new results derived for non-linear phase shifting in the Haar wavelet domain. Although image-based methods for real-time rendering of dynamic glossy objects have been proposed, they do not truly scale to all possible frequencies and high sampling rates without trading storage, glossiness, or computational time, while varying both lighting and viewpoint. This is due to the fact that current approaches are limited to precomputed radiance transfer (PRT), which is prohibitively expensive in terms of memory requirements and real-time rendering when both varying light and viewpoint changes are required together with high sampling rates for high frequency lighting of glossy material. On the other hand, current methods cannot handle object rotation, which is one of the paramount issues for all PRT methods using wavelets. This latter problem arises because the precomputed data are defined in a global coordinate system and encoded in the wavelet domain, while the object is rotated in a local coordinate system. At the root of all the above problems is the lack of efficient run-time solution to the nontrivial problem of rotating wavelets (a non-linear phase-shift), which we solve in this paper.

Index Terms

Light Integral Equation, Rendering, Image-Based Relighting, Lambertian and Phong models

I. INTRODUCTION

Image-based rendering (IBR) has been an active area of research in computational imaging and computational photography in the past two decades. It has led to many interesting non-traditional problems in image processing and computer vision, which in turn have benefited from traditional methods such as shape and scene description [3]–[5], [12], [13], [17], [18], [36], [43]–[45], [62], [64], [82]–[85], [88]–[91], [96], [98], [114], [125], [166], [168], [169], [171], [181], scene content modeling [92], [93], [97], [99]–[101], [173]–[177], super-resolution (in particular in 3D) [33]–[35], [53], [77], [81], [113], [137]–[139], [141]–[147], [150], [151], [153], video content modeling [11], [14]–[16], [19], [20], [39], [154]–[159], [167], [170], image alignment [8], [21]–[23], [25]–[28], [31], [32], [65]–[70], [72], [73], [140], [148], [149], tracking and object pose estimation [120]–[122], [152], [161], and camera motion quantification and calibration [10], [29], [46]–[48], [48]–[50], [52], [56]–[58], [71], [86], [87], [94], [95], [102]–[105], [115], to name a few.

Using images to estimate or model environment light for relighting objects introduced or rendered in a scene is a central problem in this area [6], [7], [24], [30], [51], [54], [55], [74], [124], [160], [179], [180]. This requires solving the light integral equation (also known as the rendering equation), which plays a crucial role in IBR. IBR and new view synthesis has been the subject of intensive research for the past two decades, motivated by various application areas, such as interactive entertainment (e.g. video games), 3D TV, and augmented reality, to name a few. Image-based view synthesis techniques can be broadly classified into two categories. Those that do not require 3D information, such as plenoptic methods and light-field rendering techniques [1], [119], [123], and those that use some 3D information either implicitly or explicitly, such as the depth image-based rendering (DIBR) methods [61], [80], [116], [128], [130], [135], [172]. A specific problem of interest in this area is also when it is desired to render a 3D object of interest within an environment captured by 2D image(s) - either a single image or several images like in plenoptic data. The latter methods may be dealing with only the relighting problem (image-based relighting) when the viewpoint is assumed stationary but the light changing dynamically, or as a more complex rendering and relighting problem, when the viewpoint is also changing due to translations and rotations [2], [111], [126], [127], [129], [131], [134]. This latter category of problems may be referred to as Physics Image Based Rendering techniques (PIBR), since they start by modeling the problem as that of solving the light transport equation. A major issue in many of these IBR problems is the amount of storage and bandwidth needed to handle the problem of view synthesis. Most methods in all the categories defined above are based on some level of precomputed information, which often requires also dealing with various issues related to the coding problem [75], [117], [123] to tackle storage and bandwidth.

The demand for photorealism in image-based rendering and relighting has been increasing in all the various categories of methods highlighted above. Parallel to photorealism, coding and compression have been extensively studied and tackled primarily as off-line issues. In this paper, we are proposing a run-time solution to PIBR that tackles the bandwidth and storage issues by solving a non-linear phase-shifting problem in the Haar domain. As such, since memory and bandwidth requirements

Mais Alnasser was with the Department of Computer Science, University of Central Florida, Orlando, FL, 32816 USA at the time this project was conducted. (e-mail: nasserm@cs.ucf.edu).

Hassan Foroosh is with the Department of Computer Science, University of Central Florida, Orlando, FL, 32816 USA (e-mail: foroosh@cs.ucf.edu).

are addressed at the run time, our solution provides a means of reducing these requirements by trading them against computation during the rendering process. Furthermore, our solution provides this advantage by directly working in the compressed domain (Haar domain), thereby making it possible to achieve the above goal with little computational overhead. In order to better understand the challenges we first review the methods in the area of PIBR.

Early attempts to PIBR have been mainly concerned with realistic rendering. Phong [132], Cook and Torrance [60], and Blinn [37] generated glossy highlights from point sources by using general specular reflection functions that are concentrated near the mirror direction. Cook, Carpenter and Porter [59] used distributed ray tracing to model glossy reflections for a specular reflection function and an arbitrary light distribution. Blinn and Newell were the first to include the light coming from the whole environment using environment maps to create mirror reflections [38]. Kajiya [106] introduced the *Rendering Equation*, which provided a unified framework for rendering different types of materials and became thereafter the focus of research for the rendering community.

There has been a remarkable progress in the last few years in finding efficient ways of solving the PIBR problem. The most recent approaches have been focusing on projecting the problem into the frequency domain such as the Spherical Harmonics or the Haar transform domain. PIBR techniques that use Haar wavelets for representation rely highly on preprocessing of data. Ng et. al. [127] discretize BRDFs along the possible orientations of the normal direction. This amounts to 6-dimensional BRDFs and gigabytes of storage. Wang et. al. [178] provide an alternative solution to rotating Haar-transformed data using geometry maps. They preprocess and store the rotation matrices instead of the BRDFs. However, their method relies on discretizing the space of possible normal orientations and interpolating between the rotation matrices at those sample directions. We provide an analytic solution that offers the option of computing rotated Haar-transformed data directly, using only the high frequency coefficients of the original data without having to resort to discretization, storage, interpolation of data, or trading off the bandwidth.

Computer systems and Graphic cards are becoming faster and more powerful. They are also becoming increasingly more capable in terms of memory. In rendering applications that favor real or interactive time, memory is often traded for speed. This essentially relies on preprocessing, which in turn relies on discretizing the data as finely as the memory would allow. However, no matter how large the size of the memory, there is always a limit to the resolution of discretization, beyond which one has to approximate the values between samples using interpolation. This is the natural effect of discretization. At the rate the speed of systems is increasing, applications have started favoring adding more computation during render time to achieve more precision - a trend in the graphics hardware community that also favors our solution for the PIBR problem.

Our run-time rendering and relighting solution requires rotating Haar wavelets, which amounts to a non-linear phase-shifting directly in the Haar wavelet domain. In a previous work [9], we proposed a solution for linear phase-shifting of multi-dimensional non-separable Haar wavelets. In this paper, we present an innovative method for non-linear phase-shifting that takes advantage of our earlier results in [9]. This is possible since the non-linear phase-shifting of the two-dimensional signals in our case are induced by linear phase shifts of three-dimensional functions defined on a unit sphere. In other words, the non-linear phase-shifting in the two-dimensional signal is a rotation of the three-dimensional data it represents.

In the remaining of this paper, we first provide a brief introduction to PIBR followed by a review of some of the most recent research in this area that are related to our work. We then present a summary of our contributions, followed by a detailed description of non-linear phase-shifting of the 2D non-separable Haar wavelets and its applications to the problem at hand. We finally provide experimental results and conclude with some remarks and discussion.

II. PHYSICS IMAGE-BASED RENDERING

As pointed out earlier, PIBR methods are based on modeling the physics of the rendering problem using the light transport integral, also known as the rendering equation. The rendering equation describes the interaction between incoming light and a surface material. The following is the most general form of the equation:

$$L_o(p, \omega_o) = L_e(p, \omega_o) + \int_{H(\vec{N})} f_r(p, \omega_o, \omega_{in}) L_{in}(p, \omega_{in}) V(p, \omega_{in}) \cos \theta_{in} d\omega_{in} \quad (1)$$

where,

- ω_o is the outgoing direction.
- $L_e(p, \omega_o)$ is the emitted light at point p in the direction ω_o .
- $L_o(p, \omega_o)$ is the radiance leaving the surface at a point p in the direction ω_o .
- $f_r(p, \omega_o, \omega_{in})$ is the Bidirectional Reflectance Distribution Function (BRDF).
- $L_{in}(p, \omega_{in})$ is the incident radiance.
- θ_{in} is the angle between the unit normal \vec{N} at the point p and ω_{in} .
- $V(p, \omega_{in})$ is the function that describes the visibility at point p along direction ω_{in} .
- $H(\vec{N})$ is the hemisphere of directions around the normal \vec{N} .

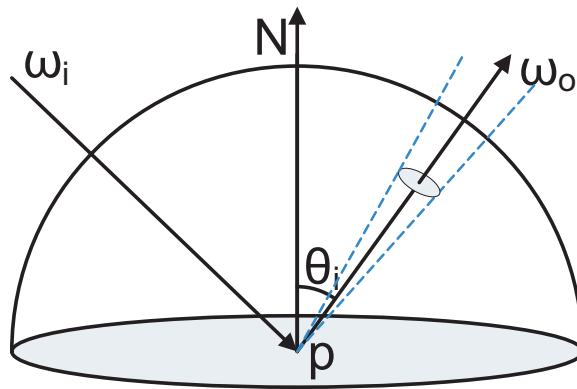


Fig. 1. Relationship between the incident light and the light leaving a point on an object surface.

Put in words, the rendering equation integrates the product of the three contributing factors of incoming light, BRDF, and the visibility function along all incident light directions. Figure 1 shows the relationship between the incident light and the reflected light off the surface of an object at a given point.

III. CLOSELY RELATED WORKS

We describe below three categories of work that are closely related to our paper, most notably the methods working in the transform domain.

A. MONTE CARLO

One of the oldest and most straightforward approaches for solving the light integral equation is to approximate the solution using the Monte Carlo method [63], [106], [107]. Global illumination algorithms based on Monte Carlo are general enough to allow estimation of the integral for any material type and light distribution.

Monte Carlo is a numerical integration method that uses sampling to estimate an average solution for integration of any dimension. This is applicable to the lighting integral because the product of the light, reflection and visibility functions is too complex to evaluate using a closed-form approach.

Monte Carlo based algorithms are, however, very slow. The convergence rate for these algorithms is $O(\frac{1}{\sqrt{n}})$, where n is the number of samples taken to estimate the integral. This means that to cut the error in half, four times the number of samples must be taken. On the other hand, unless sufficient light samples are taken, Monte Carlo produces noisy results that manifest as pixels that are too bright or too dark in the rendered image. Therefore, a substantial number of samples and accordingly more time is typically required in order to render a realistic low-noise image.

Much research has gone into improving Monte Carlo's performance without increasing the number of samples. One of the techniques that has been most effective is importance sampling [2], [111], [129]. Importance sampling relies on sampling mostly in the "important" directions, which is governed by the choice of a sampling distribution function that is similar in shape to the integrand of the function that is being estimated [131].

Many attempts have been also made to speed the rendering time by splitting the scene synthesis into an offline prefiltering preprocess and a rendering process. Prefiltering stores the result of integrating the product of the BRDF and lighting over the visible upper hemisphere per normal direction. Cabral et al. [42] used prefiltering to obtain a sparse 2D set of prerendered images that were used during the rendering process to generate rendered images at interactive rates. [108] and [110] subsequently proposed alternative methods for improving prefiltering methods.

B. FREQUENCY DOMAIN

C. SPHERICAL HARMONICS

The first attempt to solve the integral in the frequency domain was by Cabral et al. [41] using *Spherical Harmonics* as basis. Spherical harmonics are the analog of the Fourier transform for representing functions on the unit sphere [118]. They are the products of *Associated Legendre Functions* with functions that are periodic with respect to the azimuth angle ϕ .

Cabral et al. [41] simplified the integral by removing the emittance and the visibility functions. They also made the assumptions that the viewing direction is fixed and that the BRDF is isotropic. They then used spherical harmonics to expand the lighting function and the product of the BRDF and the cosine function, with the viewing direction as the north pole. Projecting the terms of the integral into the spherical harmonics space reduces the integration into an inner product because of the orthonormality of spherical harmonics.

The next use of spherical harmonics was by Sillion et al. [162] to represent exit radiance at many points in a progressive radiosity simulation. They provide a general off-line treatment of transfer functions ranging from ideal specular to ideal diffuse reflection.

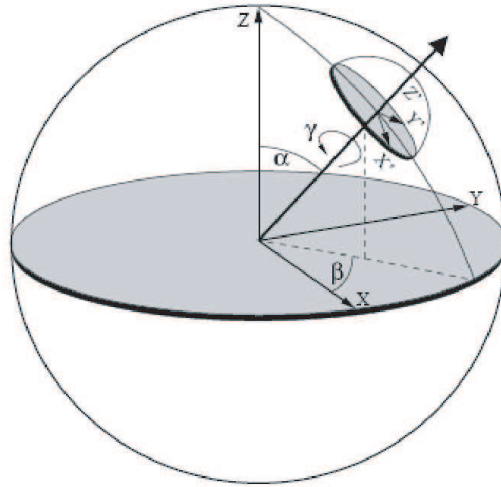


Fig. 2. The local and global coordinate systems.

Ramamoorthi and Hanrahan [134] gave explicit formulae in terms of the cartesian coordinates of the surface normal and approximated the solution of the integral for diffuse materials using 9 coefficients only. Their solution was the first to use spherical harmonics for realistic real-time rendering in the area of PIBR. Their formulae implicitly handle the required rotation of light coefficients into the local space defined by the normal as its Y-direction. This rotation is required because of the different coordinate spaces of the BRDF and the light function. The BRDF is sampled and projected into spherical harmonics' frequency domain in local space, that is, the surface normal is the Y-axis of the space. On the other hand, the light is sampled and projected in the global space, that is, the up-direction is the Y-axis of the space (see Fig. 2). Kautz et al. [109] extend the use of spherical harmonics to arbitrary BRDF's under low-frequency lighting. They represented the lighting environment using 25 coefficients and rotated them for each vertex during rendering at interactive rates. They also combined their method with Precomputed Radiance Transfer (PRT) [164] to handle interreflections and shadows. Functions represented by spherical harmonics can be rotated by a linear transformation of the representation coefficients [76]. The existing procedures [40], [78], [79], [109], however, are slow and cause a bottleneck in the rendering process. Křivánek et al. [112] propose an efficient approximation of the spherical harmonic rotation based on replacing the general spherical harmonic rotation matrix with its truncated Taylor expansion. Their proposed rotation approximation is faster and has a lower computational complexity. The approximation, however, is accurate only for small rotation angles and, therefore, applicable only to certain applications that require small successive rotation angles.

Spherical harmonics are shift-invariant, which makes them suitable for representing functions on the sphere. However, they are globally supported and, therefore, suffer from some of the same difficulties as the Fourier transform on the line such as the Gibbs phenomenon. Furthermore, spherical harmonics don't have good localization, which means a large number of coefficients is required for representing high frequency functions. Also, to handle the visibility function, it has to be combined with the BRDF and projected as one function, referred to as the *Transfer Function*, in order to be able to convert the lighting integral into an inner product. This restricts the BRDF representation in the sense that rather than having one representation for a certain material, there would be several representations of the same material, each dependant on the object occlusion properties. Furthermore, the redundancy of the BRDF information occurs per sample point per object due to the dependence of occlusion on the position of the sample point.

Imposing constraints to simplify the integral to achieve real-time or interactive rates is a necessity with spherical harmonics, when glossy or general BRDF's are used. One method is to use low sampling rates, which is equivalent to band-limiting the illumination. This approach is used by Sloan et al. in [164], [165] and [163]. However, band-limiting removes high frequency components, which blurs lighting detail. For diffuse materials, the error can be very low [134]. However, this approach is not suitable for glossy materials, which need the high frequency for an efficient representation. Another approach is to reduce the dimensionality of the problem by fixing the light or the viewing direction as in Kautz et al. [109]. This approach, however, restricts the dynamics of the scene.

D. HAAR-DOMAIN METHODS

Ng et al. [126] used non-linear wavelet approximation to achieve better localization than spherical harmonics and were successful at representing different degrees of shadowing due to wavelets' excellent capability in handling information at different scales. They, however, reduced the dimensionality of the integral to simplify it by fixing the viewing direction. Ng et al. [127] developed a method for solving the triple-product integral using two-dimensional non-separable Haar wavelets to avoid reducing the dimensionality of the problem and the low sampling rate inherent in spherical harmonics methods. to a triple product:

$$L_o(p, \omega_o) = \int_S L_{in}(p, \omega_{in}) f_r(p, \omega_o, \omega_{in}) \cos \theta_{in} V(p, \omega_{in}) d\omega_{in} \quad (2)$$

$$= \int_S L_{in}(p, \omega_{in}) \tilde{f}_r(p, \omega_o, \omega_{in}) V(p, \omega_{in}) d\omega_{in} \quad (3)$$

$$\approx \int_S \left(\sum_i a_i(p) \Psi_i(\omega_{in}) \right) \left(\sum_j b_j(p, \omega_o) \Psi_j(\omega_{in}) \right) \left(\sum_k c_k(p) \Psi_k(\omega_{in}) \right) d\omega_{in} \quad (4)$$

$$= \sum_i \sum_j \sum_k a_i(p) b_j(p, \omega_o) c_k(p) \int_S \Psi_i(\omega_{in}) \Psi_j(\omega_{in}) \Psi_k(\omega_{in}) d\omega_{in} \quad (5)$$

$$= \sum_i \sum_j \sum_k C_{ijk} a_i(p) b_j(p, \omega_o) c_k(p) \quad (6)$$

where,

$$C_{ijk} = \int_S \Psi_i(\omega_{in}) \Psi_j(\omega_{in}) \Psi_k(\omega_{in}) d\omega_{in}$$

This formulation was general and worked for any basis. However, solving for C_{ijk} and efficiently computing the triple sum in (6) was not a trivial matter. One can refer to [127] for an in-depth analysis of the computational complexity for the different methods to solve the triple sum.

Haar wavelets provide an efficient solution for solving the triple sum due to the following simple theorem [127]:

1) *The Tripling Coefficient Theorem* The integral of three 2D Haar basis functions is non-zero if and only if one of the following three cases hold:

- a) All three are scaling functions, that is, $C_{ijk} = 1$.
- b) All three occupy the same wavelet square and all are different wavelet types, that is $C_{ijk} = 2^l$, where wavelets are at level l .
- c) Two are identical wavelets, and the third is either the scaling function or a wavelet that overlaps at a strictly coarser level, that is, $C_{ijk} = \pm 2^l$, where the third function exists at level l .

The above theorem implies that most of the tripling coefficients are equal to zero because most pairs of basis functions do not overlap, which is the reason for the efficiency of using 2D Haar wavelets to solve the triple product integral.

However, Haar wavelets are not rotation-invariant, therefore, the BRDF has to be sampled per normal direction, which is storage and bandwidth intensive and has a limit on how much resolution it can afford. Furthermore, Haar wavelets are parameterized in cube domains to represent spherical functions. This makes it difficult or impossible to obtain an analytic rotation formula in the frequency domain. This is due to the representation mechanism, which compresses each face of the cube as a separate entity. To be able to rotate in the frequency domain data has to move from one face to another, which is not feasible with the cube representation.

Schröder and Sweldens [136] constructed biorthogonal wavelets on the sphere using the lifting scheme. Their method achieved better localization than spherical harmonics for high-frequency glossy materials and was defined directly on the sphere. However, it was also not rotation-invariant and did not lend itself to solving the rendering triple integral equation in an efficient manner.

Wang et al. [178] parameterized the spherical functions using geometry maps [133] and provided a solution for wavelet rotation using precomputed rotation matrices. They precomputed and stored the rotation matrices and used them to rotate the light coefficients into the local space of the BRDF. However, their solution was brute force rather than analytic, since it would be impossible to derive rotation formulae for the frequency domain with the geometry map representation.

IV. OUR CONTRIBUTIONS

Rotation directly in the Haar wavelet domain: We derive for the first time an explicit solution for rotating functions directly in the Haar wavelet domain. The key idea that allows us to achieve this result is the fact that for a standard non-separable Haar transform the horizontal, vertical, and diagonal coefficients are simply first order finite difference approximations of horizontal, vertical, and diagonal derivatives of the function at different scales. Therefore, we first derive the explicit expressions in

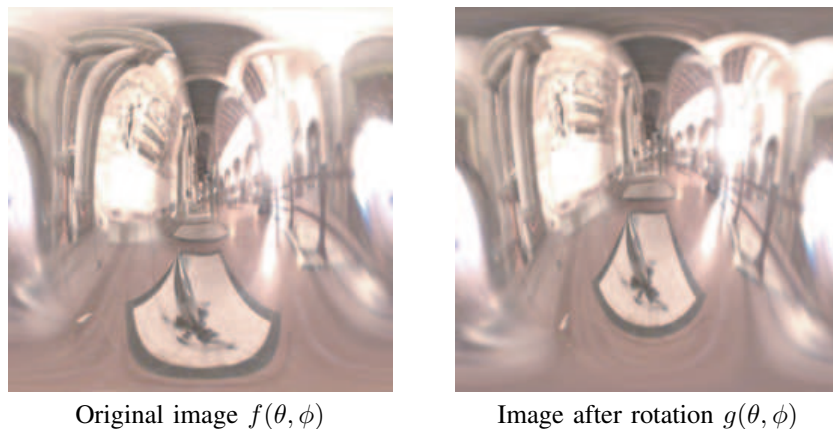


Fig. 3. An example demonstrating a non-linear phase shift that corresponds to a rotation on the unit sphere.

the spatial domain that describe rotations of a function defined over the unit sphere. Using the chain rule, and the fact that differentiation is a linear operator, we then show how the order of rotation and differentiation can be interchanged. As a result, we derive an explicit method for rotating Haar wavelets, which is essentially a non-linear phase shift in the Haar domain.

Scalable solution for light transport: Direct Haar domain rotation completely removes the precomputation burden and the overly expensive storage and bandwidth requirements, since the rotations between local and global coordinates for the BRDF, light, or visibility can be performed directly on the wavelet coefficients during run-time. Throughout this paper the term “run-time” refers to computation of the radiance transfer without performing any precomputation. We thus call our approach a run-time radiance transfer (RRT) method as opposed to PRT described above. Although, our approach provides a run-time solution, as seen below, the first algorithm derived tends to be expensive. Fortunately, however, we demonstrate that a simple reformulation of the algorithm reduces the time complexity drastically. As a result, we obtain a solution that provides run-time rotation of the Haar coefficients over the entire frequency range, without requiring any data-loss, precomputation, or extensive storage or bandwidth requirements: the rotated coefficients for the entire frequency range are computed recursively from only one level of coefficients of the Haar transform of the original map prior to rotation. Therefore, our solution does not have to sacrifice glossiness, against storage and bandwidth. We also don’t have to interpolate between preprocessed data, whether it is the data itself or the rotation matrices, which means our method is more accurate at any given rotation angle. This is important especially with high frequency information because interpolation acts as a low-pass filter.

V. OUR METHOD

As mentioned earlier, the BRDF and the light function are represented under different coordinate spaces. The BRDF is sampled and projected into frequency domain in local space, that is, the surface normal is the Y-axis of the space. On the other hand, the light is sampled and projected in global space, that is, the up-direction is the Y-axis of the space. This requires a rotation of one of the coordinate spaces into the other before the triple product can be performed. Currently, the most efficient computation of the triple product is performed in the Haar domain [127]. Thus the key to solve the problem is to devise a method for rotating directly in the Haar domain, which we describe in the next section.

A. ROTATING HAAR

We describe our solution for the light. But, it equally applies to any function defined over the unit sphere such as the visibility map or the BRDF. Our implementation, however, rotates the BRDF data from local space into global space due to its higher degree of smoothness when mapped to a two-dimensional square, which reduces errors incurred by rotation.

Let $f(\theta, \phi)$ be a function that describes the light map in a spherical coordinate system at some initial orientation¹. Our first goal here is to derive the relations that describe rotation in the spherical coordinate system (see Fig. 3 for an example). Let α_l , β_l and γ_l denote the Euler rotation angles from global to local space along the cartesian axes X , Y , and Z , respectively. Then, the light map after rotation, denoted hereafter by $g(\theta, \phi)$, can be derived in terms of $f(\theta, \phi)$ as follows:

Let \mathbf{p} denote a point in the cartesian coordinate system after rotation, i.e. $\mathbf{p} \in g(\theta, \phi)$. Then the mapping from spherical coordinates to cartesian coordinates is given by:

$$\mathbf{p} = \begin{bmatrix} x \\ y \\ z \end{bmatrix} = \begin{bmatrix} \sin \theta \sin \phi \\ \cos \theta \\ \sin \theta \cos \phi \end{bmatrix}$$

¹We do not explicitly include the radius in spherical coordinates to imply that we are dealing with mappings over a unit sphere.

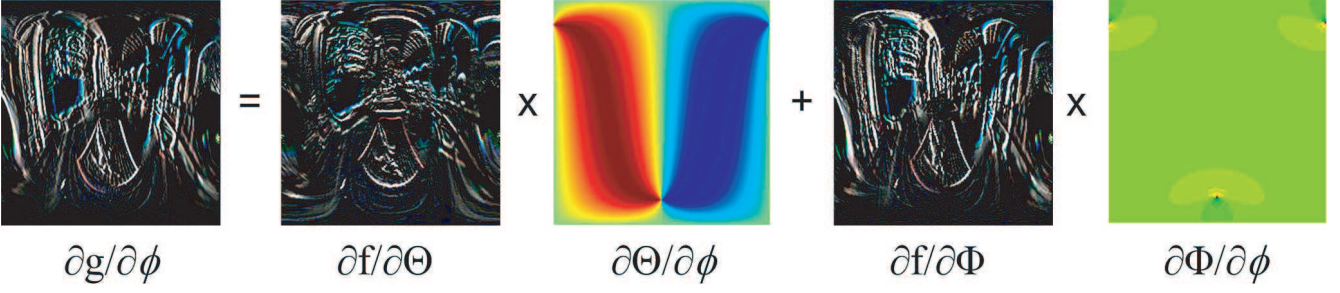


Fig. 4. This figure shows an example of evaluating $\frac{dg}{d\phi}$ in equation (13) after a rotation along the elevation angle by 20° .

where we assume a right-handed global coordinate system, with the Y -axis pointing up and the Z -axis representing the depth. The position of the point prior to an arbitrary rotation $\mathbf{R} \in f(\theta, \phi)$ is determined by the following matrix equation:

$$\mathbf{p}' = \mathbf{R}_z \mathbf{R}_y \mathbf{R}_x \mathbf{p} = \mathbf{R} \mathbf{p} \quad (7)$$

where \mathbf{R}_x , \mathbf{R}_y and \mathbf{R}_z are the familiar rotation matrices along the corresponding X , Y and Z axes. For brevity, we can write the elements of \mathbf{p}' as follows:

$$\mathbf{p}' = \begin{bmatrix} \mathbf{R}_1 \mathbf{p} \\ \mathbf{R}_2 \mathbf{p} \\ \mathbf{R}_3 \mathbf{p} \end{bmatrix} \quad (8)$$

where $\mathbf{R}_i, i = 1, \dots, 3$ are the rows of the rotation matrix \mathbf{R} .

Assuming that the point prior to rotation has an elevation angle of θ' and an azimuth angle of ϕ' , we can readily verify that

$$g(\theta, \phi) = f(\theta', \phi')$$

where

$$\theta' = \cos^{-1}(\mathbf{R}_2 \mathbf{p}) \quad (9)$$

$$\phi' = \tan^{-1}\left(\frac{\mathbf{R}_1 \mathbf{p}}{\mathbf{R}_3 \mathbf{p}}\right) \quad (10)$$

Unfortunately, one can easily see from the above relations that the rotation is not a linear operation in the spherical coordinate system. In other words, θ' and ϕ' are not linearly related to θ and ϕ . The key observation that allows us to solve the problem is that we are specifically dealing with Haar transform coefficients, which correspond to the first order finite difference approximations of the horizontal, vertical and diagonal derivatives of the map $f(\theta, \phi)$ at different resolution levels (scales).

Therefore, let $\theta' = \Theta(\theta, \phi)$ and $\phi' = \Phi(\theta, \phi)$, denote the non-linear mappings that relate the elevation and azimuth angles before and after rotation, as given by (9) and (10). Then

$$g(\theta, \phi) = f(\Theta(\theta, \phi), \Phi(\theta, \phi)) \quad (11)$$

The horizontal, vertical and diagonal derivatives are essentially the derivatives with respect to the angles ϕ , θ and $\phi\theta$, respectively. The illuminating feature of (11) is that it indicates that the solution to our problem lies simply in the chain rule:

$$\frac{dg}{d\theta} = \frac{\partial f}{\partial \Theta} \frac{\partial \Theta}{\partial \theta} + \frac{\partial f}{\partial \Phi} \frac{\partial \Phi}{\partial \theta} \quad (12)$$

$$\frac{dg}{d\phi} = \frac{\partial f}{\partial \Theta} \frac{\partial \Theta}{\partial \phi} + \frac{\partial f}{\partial \Phi} \frac{\partial \Phi}{\partial \phi} \quad (13)$$

$$\begin{aligned} \frac{d^2 g}{d\phi d\theta} &= \frac{\partial^2 f}{\partial \Theta \partial \theta} \frac{\partial \Theta}{\partial \theta} + \frac{\partial^2 f}{\partial \Theta} \frac{\partial^2 \Theta}{\partial \phi \partial \theta} \\ &+ \frac{\partial^2 f}{\partial \Phi \partial \theta} \frac{\partial \Phi}{\partial \phi} + \frac{\partial f}{\partial \Phi} \frac{\partial^2 \Phi}{\partial \phi \partial \theta} \end{aligned} \quad (14)$$

We concur from the above that finding the horizontal, vertical and diagonal Haar coefficients after some rotation reduces to the problem of applying the chain rule to the coefficients of the Haar transform of f prior to rotation - achieving, thus, rotation of the coefficients directly in the transform domain. Again, this is true because Haar coefficients conveniently correspond to function derivatives at different scales. Figure 4 shows an example of computing $\frac{dg}{d\phi}$ after a vertical elevation of $\alpha_l = 20^\circ$,

where $\frac{\partial f}{\partial \Theta}$ and $\frac{\partial f}{\partial \Phi}$ are obtained from the vertical coefficients $\frac{\partial f}{\partial \theta}$ and the horizontal coefficients $\frac{\partial f}{\partial \phi}$, respectively, through an elevation by the same angle.

This provides an elegant analytic solution to the rotation of Haar wavelets defined over a spherical coordinate system. Furthermore, our method can be applied to any map other than the longitude-latitude map as long as there exists a mathematical expression that maps the data from the sphere to all pixels of a rectangular image. In other words, if $\Theta(\theta, \phi)$ and $\Phi(\theta, \phi)$ can be explicitly expressed mathematically then our method for rotation can be used for spherical data represented using that map.

Taking advantage of the longitude-latitude map, one can reduce the complexity of the rotation matrix \mathbf{R} . Assuming that a rotation by θ_l along the elevation angle is aligned with the rotation around the X-axis, then θ_l equals α_l . This in turn means that a rotation by θ_l can be represented by \mathbf{R}_x . A rotation with respect to the azimuth angle by ϕ_l simply becomes a linear shift of the elevated point. This reduces \mathbf{R} from a multiplication of the three euler rotation matrices to one matrix and a linear shift. This significantly reduces the number of cosine and sine terms in \mathbf{R} and, therefore, reducing its complexity.

B. MATHEMATICAL DESCRIPTION

The basic idea here is that the Haar coefficients at any level $j+1$ of a function f defined over the spherical coordinates can be considered as the horizontal, vertical and the diagonal derivatives of f with respect to the elevation and azimuth angles at that level (scale). Therefore, given the Haar coefficients of f at level $j+1$, we can directly compute the derivatives $g_\theta(\theta, \phi) = \frac{dg}{d\theta}$, $g_\phi(\theta, \phi) = \frac{dg}{d\phi}$, and $g_{\theta\phi}(\theta, \phi) = \frac{d^2g}{d\phi d\theta}$ of the rotated function g at level $j+1$ by simply using the equations (12)-(14). To obtain the Haar coefficients of g at level j , we simply need to convolve these derivatives with 2×2 averaging kernels and then downsample the results.

Simple inspection then shows that Haar coefficient at all coarser levels $j-1, j-2, j-3, \dots$ can be computed directly from the derivatives g_θ, g_ϕ , and $g_{\theta\phi}$ by a series of convolutions and downsampling. We describe the main idea using the vertical coefficients as an example. Suppose we want to compute the vertical coefficients v_{j-l} at level $j-l$ using the vertical derivatives g_θ . This amounts to convolving the vertical derivatives with two separate kernels as follows:

$$v_{j-l}(\theta, \phi) = \sum_{\rho} h_{s,j-l}(\rho - \phi) \sum_{\tau} g_\theta(\theta, \phi) h_{t,j-l}(\tau - \theta) \quad (15)$$

where

$$h_{t,j-l}(\theta) = \left(2^{l+1} - |\theta|\right) \quad , \quad \theta \in [-2^{l+1} + 1, 2^{l+1} - 1] \quad (16)$$

and

$$h_{s,j-l}(\phi) = \frac{1}{2^{l+2}} \quad , \quad \phi \in [-2^{l+1} + 1, 2^{l+1} - 1] \quad (17)$$

followed by downsampling by a factor of 2^{l+2} .

Horizontal Haar coefficients at level $j-l$ can be similarly computed from g_ϕ by interchanging the role of h_t and h_s . The diagonal coefficients are simply computed by taking the cross-derivative either using the horizontal or the vertical coefficients and convolving in both directions by h_s .

C. ALGORITHMIC OPTIMIZATION

The simple but powerful results derived in the previous section show that we can directly compute the Haar coefficients of a rotated function at all levels $j-l, l = 0, 1, 2, \dots$ directly from the Haar coefficients of the original function at only one level, i.e. level $j+1$. However, it can be verified from (15)-(17) that as l increases the time complexity of (15) increases exponentially. At a first glance, this may seem disappointing, however, it turns out that this is rather misleading, and there is a simple solution to reduce the complexity to provide run-time computation.

There are two measures that we can take to optimize the algorithm: First, note that the Haar coefficients at all levels $j-l, l = 0, 1, 2, \dots$ are computed from the derivatives at level $j+1$. Second the convolution kernels $h_{t,j-l}$ and $h_{s,j-l}$ increase exponentially in size as l increases. Both problems can be alleviated by identifying the fact that the proposed computations in the previous section can be performed recursively so that at each level the computation of the Haar coefficients depends only on the Haar coefficients computed at the previous level. To this end, we note that for all $l \geq 1$, the kernel $h_{t,j-l}$ can be written as the convolution of two kernels:

$$h_{t,j-l} = h_{t,j} * h_{t,j}^l \quad (18)$$

where

$$h_{t,j}^l(\theta) = \begin{cases} h_{t,j} \left(\frac{\theta}{2^l}\right) & \text{if } \frac{\theta}{2^l} \text{ is an integer} \\ 0 & \text{otherwise} \end{cases} \quad (19)$$

Note that except for three values, all the values in the kernel $h_{t,j}^l$ are zero. Essentially, $h_{t,j}^l$ is the same kernel as $h_{t,j}$, but upsampled by a factor of 2^l , by zero padding all elements between the non-zero values. Therefore, the algorithm can be

implemented recursively by repeated convolution with the upsampled kernel $h_{t,j}^l$ for all $l \geq 1$. The latter is very cheap since except for three values all the values in the kernel are zero. Simple inspection indicates that the reduced algorithm is $O(n)$.

In addition to the above algorithmic optimization for recursive computation of the Haar coefficients, we can further reduce the computational time by modifying also the rotation step based on the chain rule described in Section V-A. To this end note that without loss of generality, we can assume that the function to be rotated is initially aligned such that the x -axis coincide with the θ -axis. The consequence of this assumption is that all rotations reduce to rotation around the θ -axis (or the x -axis) followed by a simple shifting along the ϕ -axis, which is extremely cheap (i.e. $O(1)$).

The following algorithm summarizes our method:

- For each pixel, determine the local outgoing direction and retrieve the BRDF transformed map corresponding to that direction.
- Assuming the transformed BRDF data has $0..n-1$ levels of resolution, the vertical, horizontal and diagonal coefficients at level $n-1$ are rotated by $\phi_{\vec{N}}$ and $\theta_{\vec{N}}$, which are the azimuth and elevation angles of the normal \vec{N} at the current pixel.
- The coefficients at the lower resolution levels are subsequently evaluated by recursively convolving by the filters h_s and h_t , where h_s and h_t have a size of 2 and 3 coefficients respectively.
- The rotated data is plugged in the triple integral computation.

The above algorithm has a complexity of $O(N)$, where N is the number of coefficients. One might argue that this is the same complexity as saving multiple levels of resolution of untransformed data using a mipmap [135], rotating the required level spatially and then transforming. Representing the data using a wavelet transform, however, is more compact than a mipmap, which saves storage space and bandwidth as is our goal. It is also more convenient to have the data in its transformed state so that they are readily available for use for the triple product computation.

We would also like to mention that one can start at any resolution level that is lower than $n-1$. In that case, the computational complexity is reduced to $O(N/4^k)$, where k is the number of levels removed.

VI. EXPERIMENTAL RESULTS AND DISCUSSION

Our algorithm is implemented using CUDA (“Compute Unified Device Architecture”) in combination with Cg for graphics rendering. The algorithm is implemented into the following passes:

The Cg Pass: This pass takes advantage of the interpolator and rasterizer of the graphic pipeline to output a fragment buffer that contains the interpolation information, vertex id, and object id per pixel.

The Rotation Input Pass: This pass outputs a buffer which contains the BRDF tile id and the rotation angles required per non-background pixel.

The Rotation Pass: This pass is actually divided into three passes that run concurrently to optimize speed. The three passes evaluate the horizontal, vertical and diagonal coefficients of the rotated BRDF tiles.

The Triple Integral Pass: This pass evaluates the illumination of each non-background pixel using the triple sum to render a 3D object in a scene based on the light captured by images.

One immediate question is whether the third step of run-time rotation in the Haar domain has an effect in the accuracy of the rendering of the object, and if so to what extent? To answer this question, we processed the BRDF data by rotating it in the spatial domain to generate the ground truth. We then processed the BRDF data by rotating it using our method of run-time rotation in the Haar domain. To make sure that we gather statistically meaningful information, we performed this process using five different popular models (“sphere”, “Easter”, “Venus”, “bunny”, and “cat”) and rendered them for two different types of surface material (aluminium bronze and blue metallic paint) using five different environment maps, i.e. “Galileo Tomb”, “Grace Cathedral”, “RNL” (light probe), “St. Petersburg”, and “Uffizi” gallery in Florence. We performed this over a large set of random rotations at levels 5 and 6, and measured the average PSNR. Results are shown in Tables I-IV. It can be immediately noticed that generally speaking these PSNR values are extremely high in the range of 100dB-120dB. It is worth noting that, for instance, in a typical state of the art lossy compression the PSNR is in the range 30dB-50dB. This indicates that the accuracy of run-time rotation in the Haar domain is on average 2-3 times better than the best available lossy compression. A quick inspection of these tables also suggest that the rotation accuracy decreases when performed at coarser levels of Haar, but not drastically so if we do not start at a too coarse level. Therefore, the gain in speed may justify the slight loss of accuracy up to some level of coarseness.

In order to also evaluate the level of errors in terms of the different object geometry, we computed the mean square error (MSE) averaged over a large set of random rotations for the same models, materials, and environment maps as above. The average MSE is very close to zero (see the plots in Figures 5 and 6). The figures show results from rotating the data from levels 5 and 6 and recursively evaluating the rest of the coefficients. Rotating from level 5 is slightly better because it has less accumulation error because of the smaller number of levels. The smaller the number of coefficients at a certain level the less smooth the data becomes, which causes inaccuracy due to discontinuity. Also, a simple inspection of these plots show that the MSE remains invariant to the environment map (lighting variations). This is significant because it implies that under dynamic lighting the MSE would remain invariant, and hence would not create visually disturbing noise. We then experimented with rendering different levels glossiness as a function of the bandwidth, i.e. the number of Haar coefficients used to render

TABLE I

AVERAGE PSNR FOR RENDERING DIFFERENT GEOMETRIC OBJECTS MADE OF ALUMINIUM BRONZE AND ROTATED RANDOMLY AT LEVEL 6 WITHIN DIFFERENT ENVIRONMENT MAPS.

Environment Map	Galileo	Grace	RNL	St. Petersburg	Uffizi
PSNR (dB)	110.82	110.92	111.54	110.76	111.02

TABLE II

AVERAGE PSNR FOR RENDERING DIFFERENT GEOMETRIC OBJECTS MADE OF ALUMINIUM BRONZE AND ROTATED RANDOMLY AT LEVEL 5 WITHIN DIFFERENT ENVIRONMENT MAPS.

Environment Map	Galileo	Grace	RNL	St. Petersburg	Uffizi
PSNR (dB)	111.17	111.81	112.56	111.29	111.62

TABLE III

AVERAGE PSNR FOR RENDERING DIFFERENT GEOMETRIC OBJECTS MADE OF BLUE METALLIC PAINT AND ROTATED RANDOMLY AT LEVEL 6 WITHIN DIFFERENT ENVIRONMENT MAPS.

Environment Map	Galileo	Grace	RNL	St. Petersburg	Uffizi
PSNR (dB)	104.28	104.64	104.97	104.66	104.73

TABLE IV

AVERAGE PSNR FOR RENDERING DIFFERENT GEOMETRIC OBJECTS MADE OF BLUE METALLIC PAINT AND ROTATED RANDOMLY AT LEVEL 5 WITHIN DIFFERENT ENVIRONMENT MAPS.

Environment Map	Galileo	Grace	RNL	St. Petersburg	Uffizi
PSNR (dB)	105.49	106.11	106.20	105.55	105.49

a specific material. Fig. 7 shows an example of objects with different levels of glossiness (low and high frequency lighting) and transparency rotated and rendered together within the same environment map. Figure 8 shows experimenting with three different materials, i.e. steel, blue metallic paint and aluminum bronze, as we increase the number of Haar coefficients used from 4 to 256. These experiments show that by using a fairly small number of Haar coefficients our method can produce variable levels of glossiness. Therefore, since we do not store rotated BRDF's or rotation matrices, our method is essentially a compressed-domain processing method for rendering materials at different levels of high-frequency content.

Our most important contribution is providing the first real solution to rotating Haar wavelets. Although one method of rotation already exists [178], it does so by creating a rotation matrix per discretized rotation angle. Each rotation matrix is created during a preprocess stage where each wavelet of a resolution less than or equal the required image size is rotated spatially then transformed and stored as one column of that specific rotation matrix. The rotation matrices are then used during rendering time to rotate any of the required data. This solution is computational rather than analytical, therefore, it relies on preprocessing and discretization, which produce errors due to interpolation.

We are currently able to rotate coefficients at level 4 using the GPU and at level 5 using the CPU. We recursively generate the coefficients at the coarser levels on the GPU. This is the equivalent of using 256 and 1024 coefficients for rendering respectively. Although PRT methods are capable of linearly compressing data and generating glossier materials at the current time, they still suffer from excess storage, discretization and interpolation error. It is a well-known fact that the speed of computing systems increase at a higher rate than memory, especially now that the market is focusing on parallel computing both on the CPU and GPU. In a few years time our method will be able to render using a larger number of coefficients and achieve interactive/real time.

VII. CONCLUSION

In this paper, we aspired to establish the grounds for our work by giving a brief but necessary introduction to wavelets, their different properties and the state of wavelet related research on the property of shift-invariance. Achieving shift-invariance was, up until now, the only method to achieve phase-shifting. However, that compromised other desired properties, which we wish to keep for the purposes of the environment lighting application at hand. These properties, namely, orthogonality, perfect reconstruction and localization are essential to solving the triple product that results from projecting the lighting integral terms into frequency space and, therefore, are a necessity to preserve. We present our current work for phase-shifting, which does not rely on shift-invariance and therefore preserves these important properties. Our recent work on linear phase-shifting of Haar wavelets was demonstrated in [9]. In this paper, we discussed the environment lighting problem and its relationship to Haar wavelets. Our goal is to achieve realistic image-based rendering and relighting of synthetic objects in a scene using Haar wavelets as the integration medium, while improving the efficiency in terms of storage over other methods by means of rotating

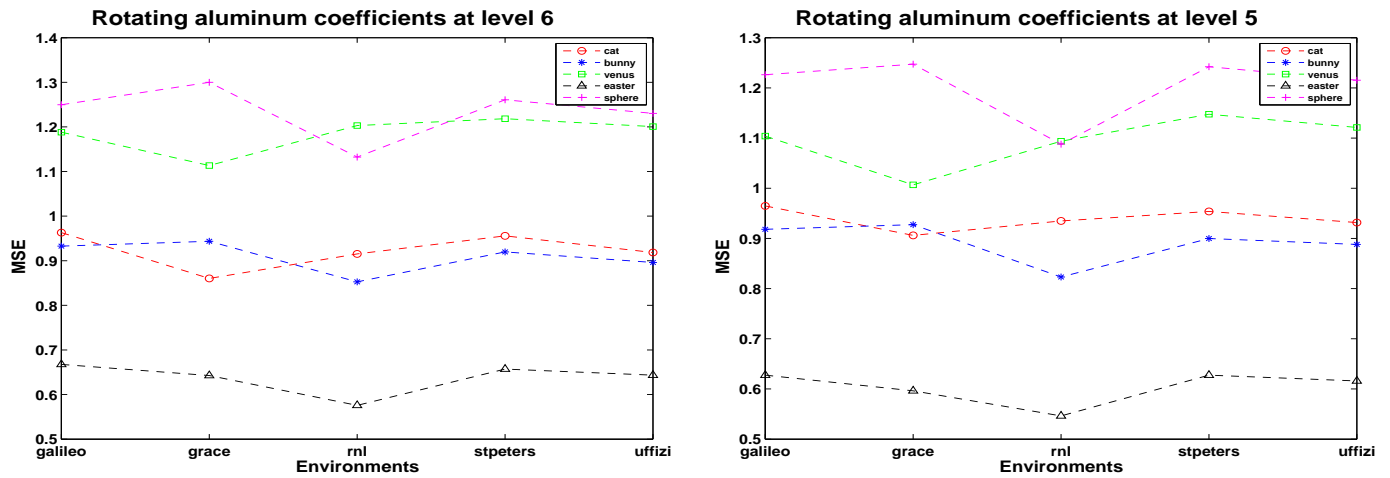


Fig. 5. The plots show the MSE, comparing rendered images of different models using aluminum bronze material under different environments. The errors are computed by comparing preprocessed data under spatial rotation with our method of rotation. Using our method, we rotated the coefficients at level 6 then evaluated the coefficients at the coarser levels, recursively.

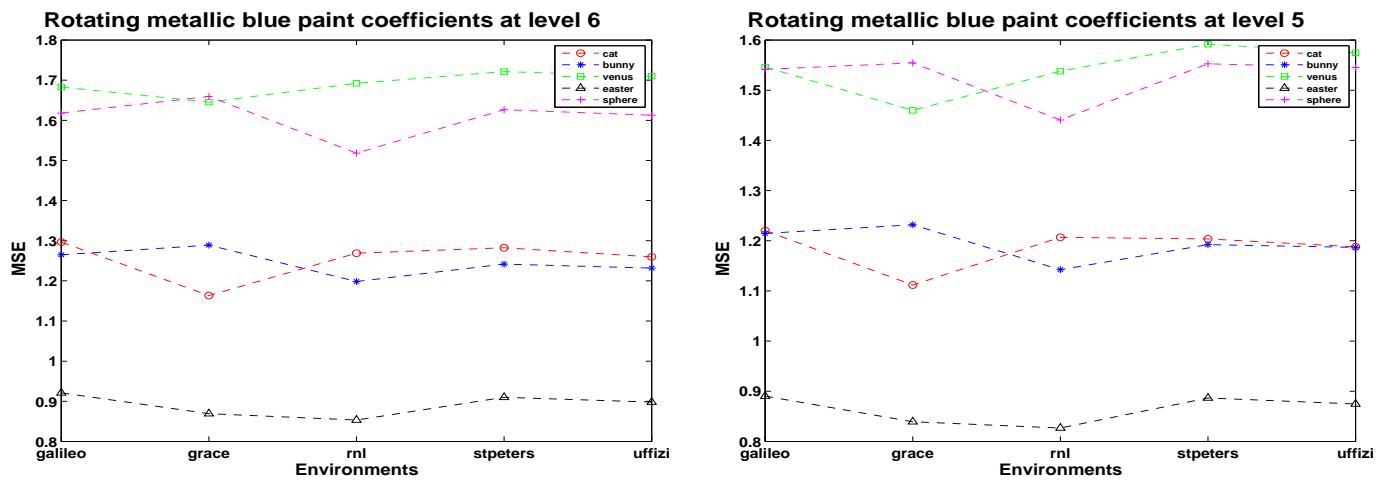


Fig. 6. The plots show the MSE, comparing rendered images of different models using blue metallic paint material under different environments. The errors are computed by comparing preprocessed data under spatial rotation with our method of rotation. Using our method, we rotated the coefficients at level 6 then evaluated the coefficients at the coarser levels, recursively.

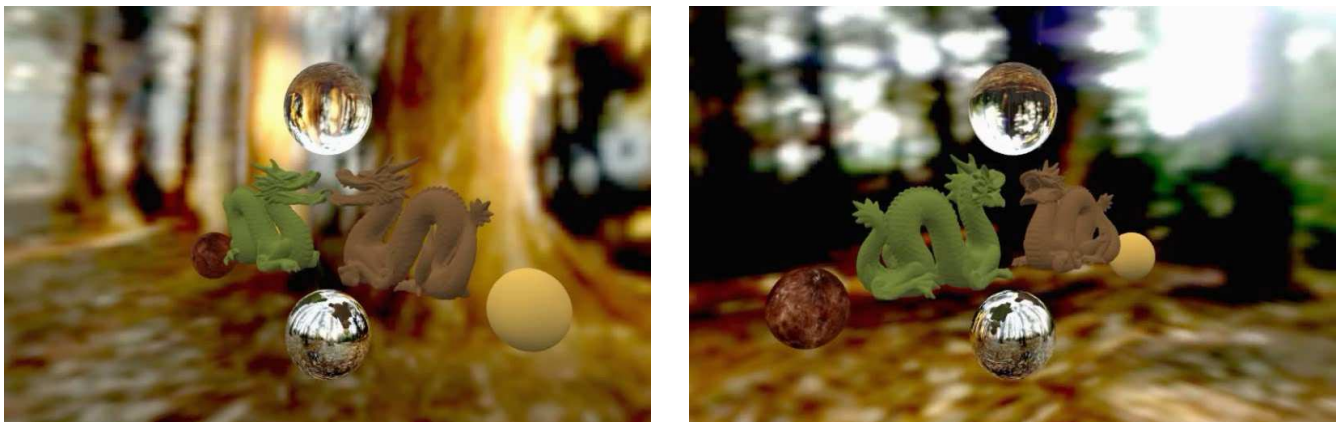


Fig. 7. Objects with different levels of glossiness (low and high frequency reflectance) and transparency rotated and rendered within the same environment map.

during rendering time. In order to do so, we devised a novel method to tackle the non-linear phase-shifting that makes use of the fact that the Haar transform implicitly contains the horizontal, vertical and diagonal derivatives of the signal. Our run-time radiance transfer method (RRT) provides an elegant solution to the non-trivial problem of rotating Haar wavelets, providing thus a solution for run-time computation of light transport based on the rendering equation. The resulting algorithm scales nicely so that no trade-off is required in terms of storage, computational cost, and bandwidth. Furthermore, since the proposed solution does not require precomputation, errors due to interpolation are avoided. Finally, our approach may be viewed as the first compressed-domain rendering method for PIBR, since all other methods in this area are storage and bandwidth intensive.



Fig. 8. Different degrees of glossiness. The rows of images are rendered with 4, 16, 64 and 256 coefficients, respectively. The three columns are rendered using steel, blue metallic paint and aluminum bronze, respectively.

REFERENCES

- [1] K. Aizawa, A. Kubota and T. Chen. Reconstructing dense light field from array of multifocus images for novel view synthesis. *IEEE Trans. Image Processing*, 16(1):269–279, 2007.
- [2] Sameer Agarwal, Ravi Ramamoorthi, Serge Belongie, and Henrik Wann Jensen. Structured importance sampling of environment maps. In *SIGGRAPH '03: ACM SIGGRAPH 2003 Papers*, pages 605–612, New York, NY, USA, 2003. ACM Press.
- [3] Muhamad Ali and Hassan Foroosh. Natural scene character recognition without dependency on specific features. In *Proc. International Conference on Computer Vision Theory and Applications*, 2015.
- [4] Muhamad Ali and Hassan Foroosh. A holistic method to recognize characters in natural scenes. In *Proc. International Conference on Computer Vision Theory and Applications*, 2016.
- [5] Muhammad Ali and Hassan Foroosh. Character recognition in natural scene images using rank-1 tensor decomposition. In *Proc. of International Conference on Image Processing (ICIP)*, pages 2891–2895, 2016.
- [6] Mais Alnasser and Hassan Foroosh. Image-based rendering of synthetic diffuse objects in natural scenes. In *Proc. IAPR Int. Conference on Pattern Recognition*, volume 4, pages 787–790, 2006.
- [7] Mais Alnasser and Hassan Foroosh. Rendering synthetic objects in natural scenes. In *Proc. of IEEE International Conference on Image Processing (ICIP)*, pages 493–496, 2006.
- [8] Mais Alnasser and Hassan Foroosh. Phase shifting for non-separable 2d haar wavelets. *IEEE Transactions on Image Processing*, 16:1061–1068, 2008.
- [9] Mais Alnasser and Hassan Foroosh. Phase-shifting for non-separable 2d haar wavelets. *IEEE Transactions on Image Processing*, 16:1061–1068, 2008.
- [10] Nazim Ashraf and Hassan Foroosh. Robust auto-calibration of a ptz camera with non-overlapping fov. In *Proc. International Conference on Pattern Recognition (ICPR)*, 2008.
- [11] Nazim Ashraf and Hassan Foroosh. Human action recognition in video data using invariant characteristic vectors. In *Proc. of IEEE Int. Conf. on Image Processing (ICIP)*, pages 1385–1388, 2012.
- [12] Nazim Ashraf and Hassan Foroosh. Motion retrieval using consistency of epipolar geometry. In *Proceedings of IEEE International Conference on Image Processing (ICIP)*, pages 4219–4223, 2015.
- [13] Nazim Ashraf, Imran Junejo, and Hassan Foroosh. Near-optimal mosaic selection for rotating and zooming video cameras. *Proc. of Asian Conf. on Computer Vision*, pages 63–72, 2007.
- [14] Nazim Ashraf, Yuping Shen, Xiaochun Cao, and Hassan Foroosh. View-invariant action recognition using weighted fundamental ratios. *Journal of Computer Vision and Image Understanding (CVIU)*, 117:587–602, 2013.
- [15] Nazim Ashraf, Yuping Shen, Xiaochun Cao, and Hassan Foroosh. View invariant action recognition using weighted fundamental ratios. *Computer Vision and Image Understanding*, 117(6):587–602, 2013.
- [16] Nazim Ashraf, Yuping Shen, and Hassan Foroosh. View-invariant action recognition using rank constraint. In *Proc. of IAPR Int. Conf. Pattern Recognition (ICPR)*, pages 3611–3614, 2010.
- [17] Nazim Ashraf, Chuan Sun, and Hassan Foroosh. Motion retrieval using low-rank decomposition of fundamental ratios. In *Proc. IEEE International Conference on Image Processing (ICIP)*, pages 1905–1908, 2012.
- [18] Nazim Ashraf, Chuan Sun, and Hassan Foroosh. Motion retrieval using low-rank decomposition of fundamental ratios. In *Image Processing (ICIP), 2012 19th IEEE International Conference on*, pages 1905–1908, 2012.
- [19] Nazim Ashraf, Chuan Sun, and Hassan Foroosh. View-invariant action recognition using projective depth. *Journal of Computer Vision and Image Understanding (CVIU)*, 123:41–52, 2014.
- [20] Nazim Ashraf, Chuan Sun, and Hassan Foroosh. View invariant action recognition using projective depth. *Computer Vision and Image Understanding*, 123:41–52, 2014.
- [21] Vildan Atalay and Hassan Foroosh. In-band sub-pixel registration of wavelet-encoded images from sparse coefficients. *Signal, Image and Video Processing*, 2017.
- [22] Vildan A. Aydin and Hassan Foroosh. Motion compensation using critically sampled dwt subbands for low-bitrate video coding. In *Proc. IEEE International Conference on Image Processing (ICIP)*, 2017.
- [23] Murat Balci, Mais Alnasser, and Hassan Foroosh. Alignment of maxillofacial ct scans to stone-cast models using 3d symmetry for backscattering artifact reduction. In *Proceedings of Medical Image Understanding and Analysis Conference*, 2006.
- [24] Murat Balci, Mais Alnasser, and Hassan Foroosh. Image-based simulation of gaseous material. In *Proc. of IEEE International Conference on Image Processing (ICIP)*, pages 489–492, 2006.
- [25] Murat Balci, Mais Alnasser, and Hassan Foroosh. Subpixel alignment of mri data under cartesian and log-polar sampling. In *Proc. of IAPR Int. Conf. Pattern Recognition*, volume 3, pages 607–610, 2006.
- [26] Murat Balci and Hassan Foroosh. Estimating sub-pixel shifts directly from phase difference. In *Proc. of IEEE International Conference on Image Processing (ICIP)*, pages 1057–1060, 2005.
- [27] Murat Balci and Hassan Foroosh. Estimating sub-pixel shifts directly from the phase difference. In *Proc. of IEEE Int. Conf. Image Processing (ICIP)*, volume 1, pages I–1057, 2005.
- [28] Murat Balci and Hassan Foroosh. Inferring motion from the rank constraint of the phase matrix. In *Proc. IEEE Conf. on Acoustics, Speech, and Signal Processing*, volume 2, pages ii–925, 2005.
- [29] Murat Balci and Hassan Foroosh. Metrology in uncalibrated images given one vanishing point. In *Proc. of IEEE International Conference on Image Processing (ICIP)*, pages 361–364, 2005.
- [30] Murat Balci and Hassan Foroosh. Real-time 3d fire simulation using a spring-mass model. In *Proc. of Int. Multi-Media Modelling Conference*, pages 8–pp, 2006.
- [31] Murat Balci and Hassan Foroosh. Sub-pixel estimation of shifts directly in the fourier domain. *IEEE Trans. on Image Processing*, 15(7):1965–1972, 2006.
- [32] Murat Balci and Hassan Foroosh. Sub-pixel registration directly from phase difference. *Journal of Applied Signal Processing-special issue on Super-resolution Imaging*, 2006:1–11, 2006.
- [33] M Berthod, M Werman, H Shekarforoush, and J Zerubia. Refining depth and luminance information using super-resolution. In *Proc. of IEEE Conf. Computer Vision and Pattern Recognition (CVPR)*, pages 654–657, 1994.
- [34] Marc Berthod, Hassan Shekarforoush, Michael Werman, and Josiane Zerubia. Reconstruction of high resolution 3d visual information. In *IEEE Conf. Computer Vision and Pattern Recognition (CVPR)*, pages 654–657, 1994.
- [35] Adeel Bhutta and Hassan Foroosh. Blind blur estimation using low rank approximation of cepstrum. *Image Analysis and Recognition*, pages 94–103, 2006.
- [36] Adeel A Bhutta, Imran N Junejo, and Hassan Foroosh. Selective subtraction when the scene cannot be learned. In *Proc. of IEEE International Conference on Image Processing (ICIP)*, pages 3273–3276, 2011.
- [37] James F. Blinn. Models of light reflection for computer synthesized pictures. pages 103–109, 1998.
- [38] James F. Blinn and Martin E. Newell. Texture and reflection in computer generated images. *Commun. ACM*, 19(10):542–547, 1976.
- [39] Hakan Boyraz, Syed Zain Masood, Baoyuan Liu, Marshall Tappen, and Hassan Foroosh. Action recognition by weakly-supervised discriminative region localization.

- [40] Choi C., Ivanic J., Gordon M., and Ruedenberg K. Rapid and stable determination of rotation matrices between spherical harmonics by direct recursion. *The Journal of Chemical Physics* 111, 19:8825–8831, November 1999.
- [41] Brian Cabral, Nelson Max, and Rebecca Springmeyer. Bidirectional reflection functions from surface bump maps. *SIGGRAPH Comput. Graph.*, 21(4):273–281, 1987.
- [42] Brian Cabral, Marc Olano, and Philip Nemeč. Reflection space image based rendering. In *SIGGRAPH '99: Proceedings of the 26th annual conference on Computer graphics and interactive techniques*, pages 165–170, New York, NY, USA, 1999. ACM Press/Addison-Wesley Publishing Co.
- [43] Ozan Cakmakci, Gregory E. Fasshauer, Hassan Foroosh, Kevin P. Thompson, and Jannick P. Rolland. Meshfree approximation methods for free-form surface representation in optical design with applications to head-worn displays. In *Proc. SPIE Conf. on Novel Optical Systems Design and Optimization XI*, volume 7061, 2008.
- [44] Ozan Cakmakci, Brendan Moore, Hassan Foroosh, and Jannick Rolland. Optimal local shape description for rotationally non-symmetric optical surface design and analysis. *Optics Express*, 16(3):1583–1589, 2008.
- [45] Ozan Cakmakci, Sophie Vo, Hassan Foroosh, and Jannick Rolland. Application of radial basis functions to shape description in a dual-element off-axis magnifier. *Optics Letters*, 33(11):1237–1239, 2008.
- [46] X Cao and H Foroosh. Metrology from vertical objects. In *Proceedings of the British Machine Conference (BMVC)*, pages 74–1.
- [47] Xiaochun Cao and Hassan Foroosh. Camera calibration without metric information using 1d objects. In *Proc. International Conf. on Image Processing (ICIP)*, volume 2, pages 1349–1352, 2004.
- [48] Xiaochun Cao and Hassan Foroosh. Camera calibration without metric information using an isosceles trapezoid. In *Proc. International Conference on Pattern Recognition (ICPR)*, volume 1, pages 104–107, 2004.
- [49] Xiaochun Cao and Hassan Foroosh. Simple calibration without metric information using an isosceles trapezoid. In *Proc. of IAPR Int. Conf. Pattern Recognition (ICPR)*, volume 1, pages 104–107, 2004.
- [50] Xiaochun Cao and Hassan Foroosh. Camera calibration using symmetric objects. *IEEE Transactions on Image Processing*, 15(11):3614–3619, 2006.
- [51] Xiaochun Cao and Hassan Foroosh. Synthesizing reflections of inserted objects. In *Proc. IAPR Int. Conference on Pattern Recognition*, volume 2, pages 1225–1228, 2006.
- [52] Xiaochun Cao and Hassan Foroosh. Camera calibration and light source orientation from solar shadows. *Journal of Computer Vision & Image Understanding (CVIU)*, 105:60–72, 2007.
- [53] Xiaochun Cao, Wenqi Ren, Wangmeng Zuo, Xiaojie Guo, and Hassan Foroosh. Scene text deblurring using text-specific multi-scale dictionaries. *IEEE Transactions on Image Processing*, 24(4):1302–1314, 2015.
- [54] Xiaochun Cao, Yuping Shen, Mubarak Shah, and Hassan Foroosh. Single view compositing with shadows. *The Visual Computer*, 21(8-10):639–648, 2005.
- [55] Xiaochun Cao, Lin Wu, Jiangjian Xiao, Hassan Foroosh, Jigui Zhu, and Xiaohong Li. Video synchronization and its application on object transfer. *Image and Vision Computing (IVC)*, 28(1):92–100, 2009.
- [56] Xiaochun Cao, Jiangjian Xiao, and Hassan Foroosh. Camera motion quantification and alignment. In *Proc. International Conference on Pattern Recognition (ICPR)*, volume 2, pages 13–16, 2006.
- [57] Xiaochun Cao, Jiangjian Xiao, and Hassan Foroosh. Self-calibration using constant camera motion. In *Proc. of IAPR Int. Conf. Pattern Recognition (ICPR)*, volume 1, pages 595–598, 2006.
- [58] Xiaochun Cao, Jiangjian Xiao, Hassan Foroosh, and Mubarak Shah. Self-calibration from turn table sequence in presence of zoom and focus. *Computer Vision and Image Understanding (CVIU)*, 102(3):227–237, 2006.
- [59] R. L. Cook, T. Porter, and L. Carpenter. Distributed ray tracing. pages 139–147, 1988.
- [60] Robert L. Cook and Kenneth E. Torrance. A reflectance model for computer graphics. In *SIGGRAPH '81: Proceedings of the 8th annual conference on Computer graphics and interactive techniques*, pages 307–316, New York, NY, USA, 1981. ACM Press.
- [61] S. Yea D. Min and A. Vetro. Temporally consistent stereo matching using coherence function. In *Proc. 3DTV-Conference*, pages 1–4, 2010.
- [62] Kristian L Damkjer and Hassan Foroosh. Mesh-free sparse representation of multidimensional LIDAR data. In *Proc. of International Conference on Image Processing (ICIP)*, pages 4682–4686, 2014.
- [63] Philip Dutre, Kavita Bala, and Philippe Bekaert. *Advanced Global Illumination*. A. K. Peters, Ltd., Natick, MA, USA, 2002.
- [64] Farshideh Einsele and Hassan Foroosh. Recognition of grocery products in images captured by cellular phones. In *Proc. International Conference on Computer Vision and Image Processing (ICCVIP)*, 2015.
- [65] H Foroosh. Adaptive estimation of motion using generalized cross validation. In *3rd International (IEEE) Workshop on Statistical and Computational Theories of Vision*, 2003.
- [66] Hassan Foroosh. A closed-form solution for optical flow by imposing temporal constraints. In *Proc. of IEEE International Conf. on Image Processing (ICIP)*, volume 3, pages 656–659, 2001.
- [67] Hassan Foroosh. An adaptive scheme for estimating motion. In *Proc. of IEEE International Conf. on Image Processing (ICIP)*, volume 3, pages 1831–1834, 2004.
- [68] Hassan Foroosh. Pixelwise adaptive dense optical flow assuming non-stationary statistics. *IEEE Trans. on Image Processing*, 14(2):222–230, 2005.
- [69] Hassan Foroosh and Murat Balci. Sub-pixel registration and estimation of local shifts directly in the fourier domain. In *Proc. International Conference on Image Processing (ICIP)*, volume 3, pages 1915–1918, 2004.
- [70] Hassan Foroosh and Murat Balci. Subpixel registration and estimation of local shifts directly in the fourier domain. In *Proc. of IEEE International Conference on Image Processing (ICIP)*, volume 3, pages 1915–1918, 2004.
- [71] Hassan Foroosh, Murat Balci, and Xiaochun Cao. Self-calibrated reconstruction of partially viewed symmetric objects. In *Proc. IEEE Int. Conf. on Acoustics, Speech, and Signal Processing (ICASSP)*, volume 2, pages ii–869, 2005.
- [72] Hassan Foroosh and W Scott Hoge. Motion information in the phase domain. In *Video registration*, pages 36–71. Springer, 2003.
- [73] Hassan Foroosh, Josiane Zerubia, and Marc Berthod. Extension of phase correlation to subpixel registration. *IEEE Trans. on Image Processing*, 11(3):188–200, 2002.
- [74] Tao Fu and Hassan Foroosh. Expression morphing from distant viewpoints. In *Proc. of IEEE International Conference on Image Processing (ICIP)*, volume 5, pages 3519–3522, 2004.
- [75] V. Velisavljevic G. Cheung and A. Ortega. On dependent bit allocation for multiview image coding with depth-image-based rendering. *IEEE Trans. Image Processing*, 20(11):3179–3194, 2011.
- [76] Robin Green. Spherical harmonic lighting: The gritty details. Technical report, Sony Computer Entertainment America, 2003.
- [77] Wei Hu, Gene Cheung, Xin Li, and Oscar C. Au. Depth map super-resolution using synthesized view matching for depth-image-based rendering. In *IEEE International Conference on Multimedia and Expo Workshops*, pages 605–610, 2012.
- [78] Joseph Ivanic and Klaus Ruedenberg. Rotation matrices for real spherical harmonics. Direct determination by recursion. *J. Phys. Chem. A*, 100(15):6342–6347, 1996.
- [79] Joseph Ivanic and Klaus Ruedenberg. Correction: Rotation matrices for real spherical harmonics. Direct determination by recursion. *J. Phys. Chem. A*, 102(45):9099–9100, 1998.
- [80] M. Brookes J. Pearson and P.L. Dragotti. Accurate non-iterative depth layer extraction algorithm for image based rendering. In *Proc. of ICASSP*, pages 901 – 904, 2011.

- [81] Apurva Jain, Supraja Murali, Nicolene Papp, Kevin Thompson, Kye-sung Lee, Panomsak Meemon, Hassan Foroosh, and Jannick P Rolland. Super-resolution imaging combining the design of an optical coherence microscope objective with liquid-lens based dynamic focusing capability and computational methods. In *Optical Engineering & Applications*, pages 70610C–70610C. International Society for Optics and Photonics, 2008.
- [82] I Junejo, A Bhutta, and Hassan Foroosh. Dynamic scene modeling for object detection using single-class svm. In *Proc. of IEEE International Conference on Image Processing (ICIP)*, volume 1, pages 1541–1544, 2010.
- [83] Imran Junejo, Xiaochun Cao, and Hassan Foroosh. Configuring mixed reality environment. In *Proc. of IEEE International Conference on Advanced Video and Signal-based Surveillance*, pages 884–887, 2006.
- [84] Imran Junejo, Xiaochun Cao, and Hassan Foroosh. Geometry of a non-overlapping multi-camera network. In *Proc. of IEEE International Conference on Advanced Video and Signal-based Surveillance*, pages 43–48, 2006.
- [85] Imran Junejo, Xiaochun Cao, and Hassan Foroosh. Autoconfiguration of a dynamic non-overlapping camera network. *IEEE Trans. Systems, Man, and Cybernetics*, 37(4):803–816, 2007.
- [86] Imran Junejo and Hassan Foroosh. Dissecting the image of the absolute conic. In *Proc. of IEEE Int. Conf. on Video and Signal Based Surveillance*, pages 77–77, 2006.
- [87] Imran Junejo and Hassan Foroosh. Robust auto-calibration from pedestrians. In *Proc. IEEE International Conference on Video and Signal Based Surveillance*, pages 92–92, 2006.
- [88] Imran Junejo and Hassan Foroosh. Euclidean path modeling from ground and aerial views. In *Proc. International Conference on Computer Vision (ICCV)*, pages 1–7, 2007.
- [89] Imran Junejo and Hassan Foroosh. Trajectory rectification and path modeling for surveillance. In *Proc. International Conference on Computer Vision (ICCV)*, pages 1–7, 2007.
- [90] Imran Junejo and Hassan Foroosh. Using calibrated camera for euclidean path modeling. In *Proceedings of IEEE International Conference on Image Processing (ICIP)*, pages 205–208, 2007.
- [91] Imran Junejo and Hassan Foroosh. Euclidean path modeling for video surveillance. *Image and Vision Computing (IVC)*, 26(4):512–528, 2008.
- [92] Imran Junejo and Hassan Foroosh. Camera calibration and geo-location estimation from two shadow trajectories. *Computer Vision and Image Understanding (CVIU)*, 114:915–927, 2010.
- [93] Imran Junejo and Hassan Foroosh. Gps coordinates estimation and camera calibration from solar shadows. *Computer Vision and Image Understanding (CVIU)*, 114(9):991–1003, 2010.
- [94] Imran Junejo and Hassan Foroosh. Optimizing ptz camera calibration from two images. *Machine Vision and Applications (MVA)*, pages 1–15, 2011.
- [95] Imran N Junejo, Nazim Ashraf, Yuping Shen, and Hassan Foroosh. Robust auto-calibration using fundamental matrices induced by pedestrians. In *Proc. International Conf. on Image Processing (ICIP)*, volume 3, pages III–201, 2007.
- [96] Imran N. Junejo, Adeel Bhutta, and Hassan Foroosh. Single-class svm for dynamic scene modeling. *Signal Image and Video Processing*, 7(1):45–52, 2013.
- [97] Imran N Junejo, Xiaochun Cao, and Hassan Foroosh. Calibrating freely moving cameras. In *Proc. International Conference on Pattern Recognition (ICPR)*, volume 4, pages 880–883, 2006.
- [98] Imran N. Junejo and Hassan Foroosh. Trajectory rectification and path modeling for video surveillance. In *Proc. International Conference on Computer Vision (ICCV)*, pages 1–7, 2007.
- [99] Imran N. Junejo and Hassan Foroosh. Estimating geo-temporal location of stationary cameras using shadow trajectories. In *Proc. European Conference on Computer Vision (ECCV)*, 2008.
- [100] Imran N. Junejo and Hassan Foroosh. Gps coordinate estimation from calibrated cameras. In *Proc. International Conference on Pattern Recognition (ICPR)*, 2008.
- [101] Imran N Junejo and Hassan Foroosh. Gps coordinate estimation from calibrated cameras. In *Proc. International Conference on Pattern Recognition (ICPR)*, pages 1–4, 2008.
- [102] Imran N. Junejo and Hassan Foroosh. Practical ptz camera calibration using givens rotations. In *Proc. IEEE International Conference on Image Processing (ICIP)*, 2008.
- [103] Imran N. Junejo and Hassan Foroosh. Practical pure pan and pure tilt camera calibration. In *Proc. International Conference on Pattern Recognition (ICPR)*, 2008.
- [104] Imran N. Junejo and Hassan Foroosh. Refining ptz camera calibration. In *Proc. International Conference on Pattern Recognition (ICPR)*, 2008.
- [105] Imran N. Junejo and Hassan Foroosh. Using solar shadow trajectories for camera calibration. In *Proc. IEEE International Conference on Image Processing (ICIP)*, 2008.
- [106] James T. Kajiya. The rendering equation. In *SIGGRAPH '86: Proceedings of the 13th annual conference on Computer graphics and interactive techniques*, pages 143–150, New York, NY, USA, 1986. ACM Press.
- [107] Malvin H. Kalos and Paula A. Whitlock. *Monte Carlo methods. Vol. 1: basics*. Wiley-Interscience, New York, NY, USA, 1986.
- [108] Jan Kautz and Michael D. McCool. Approximation of glossy reflection with prefiltered environment maps. In *Graphics Interface*, pages 119–126, 2000.
- [109] Jan Kautz, Peter-Pike Sloan, and John Snyder. Fast, arbitrary brdf shading for low-frequency lighting using spherical harmonics. In *EGRW '02: Proceedings of the 13th Eurographics workshop on Rendering*, pages 291–296, Aire-la-Ville, Switzerland, Switzerland, 2002. Eurographics Association.
- [110] Jan Kautz, Pere-Pau Vázquez, Wolfgang Heidrich, and Hans-Peter Seidel. Unified approach to prefiltered environment maps. In *Proceedings of the Eurographics Workshop on Rendering Techniques 2000*, pages 185–196, London, UK, 2000. Springer-Verlag.
- [111] Thomas Kollig and Alexander Keller. Efficient illumination by high dynamic range images. In *EGRW '03: Proceedings of the 14th Eurographics workshop on Rendering*, pages 45–50, Aire-la-Ville, Switzerland, Switzerland, 2003. Eurographics Association.
- [112] Jaroslav Křivánek, Jaakko Konttinen, Sumanta Pattanaik, Kadi Bouatouch, and Jiří Žára. Fast approximation to spherical harmonics rotation. In *SIGGRAPH '06: ACM SIGGRAPH 2006 Sketches*, page 154, New York, NY, USA, 2006. ACM Press.
- [113] Anne Lorette, Hassan Shekarforoush, and Josiane Zerubia. Super-resolution with adaptive regularization. In *Proc. International Conf. on Image Processing (ICIP)*, volume 1, pages 169–172, 1997.
- [114] Sina Lotfian and Hassan Foroosh. View-invariant object recognition using homography constraints. In *Proc. IEEE International Conference on Image Processing (ICIP)*, 2017.
- [115] Fei Lu, Xiaochun Cao, Yuping Shen, and Hassan Foroosh. Camera calibration from two shadow trajectories. In *Proc. of IEEE International Conference on Advanced Video and Signal-based Surveillance*, volume 2.
- [116] D. Doshkov H. Lakshman P. Merkle K. Müller M. Köppel, P. Ndjiki-Nya and T. Wiegand. Temporally consistent handling of disocclusions with texture synthesis for depth-image-based rendering. In *Proc. IEEE ICIP*, pages 1809 – 1812, 2010.
- [117] Y. Shinagawa M. Maitre and M.N. Do. Wavelet-based joint estimation and encoding of depth-image-based representations for free-viewpoint rendering. *IEEE Trans. Image Processing*, 17(6):946–957, 2008.
- [118] T. M. MacRobert. *Spherical Harmonics; an elementary treatise on harmonic functions, with applications*. Dover Publications, 1948.
- [119] Leonard McMillan and Gary Bishop. Plenoptic modeling: an image-based rendering system. In *Proceedings of SIGGRAPH*, pages 39–46, 1995.
- [120] Brian Millikan, Aritra Dutta, Qiyu Sun, and Hassan Foroosh. Compressed infrared target detection using stochastically trained least squares. *IEEE Transactions on Aerospace and Electronics Systems*, page accepted, 2017.
- [121] Brian Millikan, Aritra Dutta, Nazanin Rahnavard, Qiyu Sun, and Hassan Foroosh. Initialized iterative reweighted least squares for automatic target recognition. In *Military Communications Conference, MILCOM, IEEE*, pages 506–510, 2015.

- [122] Brian A. Millikan, Aritra Dutta, Nazanin Rahnavard, Qiyu Sun, and Hassan Foroosh. Initialized iterative reweighted least squares for automatic target recognition. In *Proc. of MILICOM*, 2015.
- [123] D. Marchand-Maillet M.N. Do and M. Vetterli. On the bandwidth of the plenoptic function. *IEEE Trans. Image Processing*, 21(2):708–717, 2012.
- [124] Brendan Moore, Marshall Tappen, and Hassan Foroosh. Learning face appearance under different lighting conditions. In *Proc. IEEE Int. Conf. on Biometrics: Theory, Applications and Systems*, pages 1–8, 2008.
- [125] Dustin Morley and Hassan Foroosh. Improving ransac-based segmentation through cnn encapsulation. In *Proc. IEEE Conf. on Computer Vision and Pattern Recognition (CVPR)*, 2017.
- [126] Ren Ng, Ravi Ramamoorthi, and Pat Hanrahan. All-frequency shadows using non-linear wavelet lighting approximation. In *SIGGRAPH '03: ACM SIGGRAPH 2003 Papers*, pages 376–381, New York, NY, USA, 2003. ACM Press.
- [127] Ren Ng, Ravi Ramamoorthi, and Pat Hanrahan. Triple product wavelet integrals for all-frequency relighting. In *SIGGRAPH '04: ACM SIGGRAPH 2004 Papers*, pages 477–487, New York, NY, USA, 2004. ACM Press.
- [128] Ha T. Nguyen and Minh N. Do. Error analysis for image-based rendering with depth information. In *Proc. IEEE ICIP*, pages 381–384, 2006.
- [129] Victor Ostromoukhov, Charles Donohue, and Pierre-Marc Jodoin. Fast hierarchical importance sampling with blue noise properties. In *SIGGRAPH '04: ACM SIGGRAPH 2004 Papers*, pages 488–495, New York, NY, USA, 2004. ACM Press.
- [130] D. Doshkov H. Lakshman P. Merkle K. Müller P. Ndjiki-Nya, M. Köppel and T. Wiegand. Depth image-based rendering with advanced texture synthesis. In *Proc. IEEE ICME*, pages 424–429, 2010.
- [131] Matt Pharr and Greg Humphreys. *Physically Based Rendering: From Theory to Implementation*. Morgan Kaufmann Publishers Inc., San Francisco, CA, USA, 2004.
- [132] Bui Tuong Phong. Illumination for computer generated pictures. *Commun. ACM*, 18(6):311–317, 1975.
- [133] Emil Praun and Hugues Hoppe. Spherical parametrization and remeshing. In *SIGGRAPH '03: ACM SIGGRAPH 2003 Papers*, pages 340–349, New York, NY, USA, 2003. ACM Press.
- [134] Ravi Ramamoorthi and Pat Hanrahan. An efficient representation for irradiance environment maps. In *SIGGRAPH '01: Proceedings of the 28th annual conference on Computer graphics and interactive techniques*, pages 497–500, New York, NY, USA, 2001. ACM Press.
- [135] G.J. Kim S. Lee and S. Choi. Real-time depth-of-field rendering using anisotropically filtered mipmap interpolation. *IEEE Trans. on Visualization and Computer Graphics*, 15(3):453–464, 2009.
- [136] Peter Schröder and Wim Sweldens. Spherical wavelets: efficiently representing functions on the sphere. In *SIGGRAPH '95: Proceedings of the 22nd annual conference on Computer graphics and interactive techniques*, pages 161–172, New York, NY, USA, 1995. ACM Press.
- [137] H Shekarforoush. *Super-Resolution in Computer Vision*. PhD thesis, PhD Thesis, University of Nice, 1996.
- [138] H Shekarforoush, M Berthod, and J Zerubia. Sub-pixel reconstruction of a variable albedo lambertian surface. In *Proceedings of the British Machine Vision Conference (BMVC)*, volume 1, pages 307–316.
- [139] H Shekarforoush and R Chellappa. adaptive super-resolution for predator video sequences.
- [140] H Shekarforoush and R Chellappa. A multifractal formalism for stabilization and activity detection in flir sequences. In *Proceedings, ARL Federated Laboratory 4th Annual Symposium*, pages 305–309, 2000.
- [141] H Shekarforoush, R Chellappa, H Niemann, H Seidel, and B Girod. Multi-channel superresolution for images sequences with applications to airborne video data. *Proc. of IEEE Image and Multidimensional Digital Signal Processing*, pages 207–210, 1998.
- [142] Hassan Shekarforoush. *Conditioning bounds for multi-frame super-resolution algorithms*. Computer Vision Laboratory, Center for Automation Research, University of Maryland, 1999.
- [143] Hassan Shekarforoush. Noise suppression by removing singularities. *IEEE Trans. Signal Processing*, 48(7):2175–2179, 2000.
- [144] Hassan Shekarforoush. Noise suppression by removing singularities. *IEEE transactions on signal processing*, 48(7):2175–2179, 2000.
- [145] Hassan Shekarforoush, Amit Banerjee, and Rama Chellappa. Super resolution for open sar data. In *Proc. AeroSense*, pages 123–129. International Society for Optics and Photonics, 1999.
- [146] Hassan Shekarforoush, Marc Berthod, Michael Werman, and Josiane Zerubia. Subpixel bayesian estimation of albedo and height. *International Journal of Computer Vision*, 19(3):289–300, 1996.
- [147] Hassan Shekarforoush, Marc Berthod, and Josiane Zerubia. 3d super-resolution using generalized sampling expansion. In *Proc. International Conf. on Image Processing (ICIP)*, volume 2, pages 300–303, 1995.
- [148] Hassan Shekarforoush, Marc Berthod, and Josiane Zerubia. *Subpixel image registration by estimating the polyphase decomposition of the cross power spectrum*. PhD thesis, INRIA-Technical Report, 1995.
- [149] Hassan Shekarforoush, Marc Berthod, and Josiane Zerubia. Subpixel image registration by estimating the polyphase decomposition of cross power spectrum. In *Proc. IEEE Conf. Computer Vision and Pattern Recognition (CVPR)*, pages 532–537, 1996.
- [150] Hassan Shekarforoush and Rama Chellappa. Blind estimation of psf for out of focus video data. In *Image Processing, 1998. ICIP 98. Proceedings. 1998 International Conference on*, pages 742–745, 1998.
- [151] Hassan Shekarforoush and Rama Chellappa. Data-driven multi-channel super-resolution with application to video sequences. *Journal of Optical Society of America-A*, 16(3):481–492, 1999.
- [152] Hassan Shekarforoush and Rama Chellappa. A multi-fractal formalism for stabilization, object detection and tracking in flir sequences. In *Proc. of International Conference on Image Processing (ICIP)*, volume 3, pages 78–81, 2000.
- [153] Hassan Shekarforoush, Josiane Zerubia, and Marc Berthod. Denoising by extracting fractional order singularities. In *Proc. of IEEE International Conf. on Acoustics, Speech and Signal Processing (ICASSP)*, volume 5, pages 2889–2892, 1998.
- [154] Yuping Shen, Nazim Ashraf, and Hassan Foroosh. Action recognition based on homography constraints. In *Proc. of IAPR Int. Conf. Pattern Recognition (ICPR)*, pages 1–4, 2008.
- [155] Yuping Shen and Hassan Foroosh. View-invariant action recognition using fundamental ratios. In *Proc. IEEE Conference on Computer Vision and Pattern Recognition (CVPR)*, pages 1–6, 2008.
- [156] Yuping Shen and Hassan Foroosh. View invariant action recognition using fundamental ratios. In *Proc. IEEE Conference on Computer Vision and Pattern Recognition (CVPR)*, 2008.
- [157] Yuping Shen and Hassan Foroosh. View-invariant recognition of body pose from space-time templates. In *Proc. of IEEE Conf. on Computer Vision and Pattern Recognition*, pages 1–6, 2008.
- [158] Yuping Shen and Hassan Foroosh. View invariant recognition of body pose from space-time templates. In *Proc. IEEE Conference on Computer Vision and Pattern Recognition (CVPR)*, 2008.
- [159] Yuping Shen and Hassan Foroosh. View-invariant action recognition from point triplets. *IEEE Transactions on Pattern Analysis and Machine Intelligence (PAMI)*, 31(10):1898–1905, 2009.
- [160] Yuping Shen, Fei Lu, Xiaochun Cao, and Hassan Foroosh. Video completion for perspective camera under constrained motion. In *Proc. of IAPR Int. Conf. Pattern Recognition (ICPR)*, volume 3, pages 63–66, 2006.
- [161] Chen Shu, Luming Liang, Wenzhang Liang, and Hassan Foroosh. 3d pose tracking with multitemplate warping and sift correspondences. *IEEE Trans. on Circuits and Systems for Video Technology*, 26(11):2043–2055, 2016.
- [162] Francis X. Sillion, James R. Arvo, Stephen H. Westin, and Donald P. Greenberg. A global illumination solution for general reflectance distributions. In *SIGGRAPH '91: Proceedings of the 18th annual conference on Computer graphics and interactive techniques*, pages 187–196, New York, NY, USA, 1991. ACM Press.

- [163] Peter-Pike Sloan, Jesse Hall, John Hart, and John Snyder. Clustered principal components for precomputed radiance transfer. In *SIGGRAPH '03: ACM SIGGRAPH 2003 Papers*, pages 382–391, New York, NY, USA, 2003. ACM Press.
- [164] Peter-Pike Sloan, Jan Kautz, and John Snyder. Precomputed radiance transfer for real-time rendering in dynamic, low-frequency lighting environments. In *SIGGRAPH '02: Proceedings of the 29th annual conference on Computer graphics and interactive techniques*, pages 527–536, New York, NY, USA, 2002. ACM Press.
- [165] Peter-Pike Sloan, Xinguo Liu, Heung-Yeung Shum, and John Snyder. Bi-scale radiance transfer. *ACM Trans. Graph.*, 22(3):370–375, 2003.
- [166] Chuan Sun and Hassan Foroosh. Should we discard sparse or incomplete videos? In *Proceedings of IEEE International Conference on Image Processing (ICIP)*, pages 2502–2506, 2014.
- [167] Chuan Sun, Imran Junejo, and Hassan Foroosh. Action recognition using rank-1 approximation of joint self-similarity volume. In *Proc. IEEE International Conference on Computer Vision (ICCV)*, pages 1007–1012, 2011.
- [168] Chuan Sun, Imran Junejo, and Hassan Foroosh. Motion retrieval using low-rank subspace decomposition of motion volume. In *Computer Graphics Forum*, volume 30, pages 1953–1962. Wiley, 2011.
- [169] Chuan Sun, Imran Junejo, and Hassan Foroosh. Motion sequence volume based retrieval for 3d captured data. *Computer Graphics Forum*, 30(7):1953–1962, 2012.
- [170] Chuan Sun, Imran Junejo, Marshall Tappen, and Hassan Foroosh. Exploring sparseness and self-similarity for action recognition. *IEEE Transactions on Image Processing*, 24(8):2488–2501, 2015.
- [171] Chuan Sun, Marshall Tappen, and Hassan Foroosh. Feature-independent action spotting without human localization, segmentation or frame-wise tracking. In *Proc. of IEEE Conference on Computer Vision and Pattern Recognition (CVPR)*, pages 2689–2696, 2014.
- [172] P. Frossard T. Maugey and G. Cheung. Consistent view synthesis in interactive multiview imaging. In *Proc. IEEE ICIP*, 2012.
- [173] Amara Tariq and Hassan Foroosh. Scene-based automatic image annotation. In *Proc. of IEEE International Conference on Image Processing (ICIP)*, pages 3047–3051, 2014.
- [174] Amara Tariq and Hassan Foroosh. Feature-independent context estimation for automatic image annotation. In *Proceedings of the IEEE Conference on Computer Vision and Pattern Recognition (CVPR)*, pages 1958–1965, 2015.
- [175] Amara Tariq, Asim Karim, and Hassan Foroosh. A context-driven extractive framework for generating realistic image descriptions. *IEEE Transactions on Image Processing*, 26(2):619–632, 2002.
- [176] Amara Tariq, Asim Karim, and Hassan Foroosh. Nelasso: Building named entity relationship networks using sparse structured learning. *IEEE Trans. on Pattern Analysis and Machine Intelligence*, 2017.
- [177] Amara Tariq, Asim Karim, Fernando Gomez, and Hassan Foroosh. Exploiting topical perceptions over multi-lingual text for hashtag suggestion on twitter. In *The Twenty-Sixth International FLAIRS Conference*, 2013.
- [178] R. Wang, R. Ng, D. Luebke, and G. Humphreys. Efficient wavelet rotation for environment map rendering. In *Proceedings of the Eurographics Symposium on Rendering*, 2006.
- [179] Jiangjian Xiao, Xiaochun Cao, and Hassan Foroosh. 3d object transfer between non-overlapping videos. In *Proc. of IEEE Virtual Reality Conference*, pages 127–134, 2006.
- [180] Jiangjian Xiao, Xiaochun Cao, and Hassan Foroosh. A new framework for video cut and paste. In *Proc. of Int. Conf. on Multi-Media Modelling Conference Proceedings*, pages 8–pp, 2006.
- [181] Changqing Zhang, Xiaochun Cao, and Hassan Foroosh. Constrained multi-view video face clustering. *IEEE Transactions on Image Processing*, 24(11):4381–4393, 2015.